

Two-Dimensional Oxide and Hydroxide Nanosheets: Controllable High-Quality Exfoliation, Molecular Assembly, and Exploration of Functionality

Published as part of the *Accounts of Chemical Research* special issue "2D Nanomaterials beyond Graphene".

Renzhi Ma and Takayoshi Sasaki*

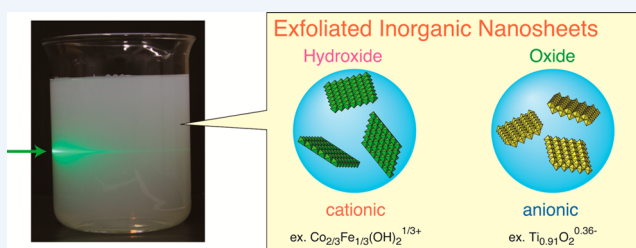
International Center for Materials Nanoarchitectonics, National Institute for Materials Science, 1-1 Namiki, Tsukuba, Ibaraki 305-0044, Japan

CONSPECTUS: Two-dimensional (2D) materials, represented by graphene, have attracted tremendous interest due to their ultimate structural anisotropy and fascinating resultant properties. The search for 2D material alternatives to graphene, molecularly thin with diverse composition, structure, and functionality, has become a hot research topic. A wide variety of layered metal oxides and hydroxides have been exfoliated into the form of individual host layers, that is, 2D nanosheets. This Account presents an overview of 2D oxide and hydroxide nanosheets on the following subtopics: (1) controllable preparation of high-quality nanosheets and (2) molecular assembly and the exploration of functionality of the nanosheets.

High-quality exfoliation is generally achieved via a multistep soft chemical process, comprised of ion-exchange, osmotic swelling, and exfoliation. A high degree of hydration-induced swelling, typically triggered by intercalation of organo-ammonium ions, is a critical stage leading to the high-yield production of molecularly thin nanosheets. Recent studies reveal that massive swelling, an astounding ~ 100 times the original size, can be induced by a range of amine solutions. The degree of swelling is controlled by the balance of osmotic pressure between the inner gallery and the outer electrolyte solution, which is strongly influenced by amine molarity. Conversely, the stability of the resultant swollen structure is dependent on the chemical nature of the amine/ammonium ions. Particular species of lower polarity and bulky size, for example, quaternary ammonium ions, are beneficial in promoting exfoliation.

Rational design and tuning of the lateral dimension, chemical composition, and structure of nanosheets are vital in exploring diverse functionalities. The lateral dimension of the nanosheets can be tuned by controlling the crystal size of the parent layered compounds, as well as the kinetics of the exfoliating reaction, for example, the type of amine/ammonium ions, their concentration, and the mode of exfoliation (manual versus mechanical shaking, etc.). Employing optimum conditions enables the production of high-quality nanosheets with a lateral size as large as several tens of micrometers. A couple of examples tailoring the nanosheets have been demonstrated with a highlight on a novel class of 2D perovskite-type oxide nanosheets with a finely tuned composition and a progressively increasing thickness at a step of 0.4–0.5 nm (corresponding to the height of the MO_6 octahedron).

The charge-bearing nanosheets can be organized through solution-based molecular assembly techniques (e.g., electrostatic layer-by-layer deposition, Langmuir–Blodgett method) to produce highly organized nanofilms, superlattices, etc., the exploration of which holds great potential for the development of various electronic and optical applications, among others.



1. INTRODUCTION

The seminal isolation and identification of graphene, a single layer of carbon atoms arranged in a two-dimensional (2D) honeycomb lattice, through the Scotch-tape micromechanical cleavage of graphite, as well as the subsequent discovery of its extraordinary mechanical, electronic, and optical properties, have triggered tremendous interest in both academia and industry.^{1,2} As a result, graphene has been proposed and widely explored for use in various applications, ranging from hybrid materials, energy conversion and storage systems, to next-generation electronic and optical devices, such as transistors, sensors, detectors, etc.^{2,3} Nevertheless, graphene is a simple

material composed of only one element, carbon. This aspect somewhat limits the versatility, as well as the tunability, of the composition, structure, and functionality.

The search for alternative 2D materials, molecularly thin with greater flexibility and diversity of composition, structure, and functionality, has become a hot research topic.^{4–7} For example, 2D materials produced from layered metal dichalcogenides, a class of van der Waals layered compounds analogous to

Special Issue: 2D Nanomaterials beyond Graphene

Received: August 21, 2014

Published: December 9, 2014

graphite, have been explored intensively. Upon exfoliation, single-layer metal dichalcogenide nanosheets exhibit attractive properties for use in nanoelectronics, optoelectronics, catalysis, etc.^{8–10} In particular, although few-layer MoS₂ is an indirect semiconductor (~1.0 eV), it becomes a direct bandgap semiconductor (~1.8 eV) in the single-layer form.^{10,11} Such semiconducting nanosheets, with direct and narrow gap, are regarded as among the most promising 2D candidate materials beyond graphene, which exhibits a peculiar Dirac cone band structure with a zero gap.

On the other hand, inorganic nanosheets derived from layered transition metal oxides and hydroxides have tunable properties, stemming from an overwhelming diversity of chemical composition and crystal structure.^{12–19} A wide range of oxide nanosheets of various transition metals have been synthesized to date. Those based on Ti, Nb, Ta, etc. are typically wide gap semiconductors (3–5 eV) while those based on Mn, Mo, W, etc., show facile redox activity.^{12,14} Generally, these oxide nanosheets exhibit high chemical and thermal stability. The potential applications of oxide nanosheets have been demonstrated in high-*k* dielectrics, magneto-optics, optoelectronics, photocatalysts, etc.^{15,16} As with oxide nanosheets, the incorporation of transition metal (Fe, Co, Ni, Zn, etc.) and rare-earth elements (RE; Ce, Eu, Gd, Tb, Er, etc.) into hydroxide nanosheets may produce interesting electronic, magnetic, and catalytic properties and thus attracts more and more research attention.^{13,14,17,18}

Single-layer oxide and hydroxide nanosheets have been systematically studied earlier, before the emergence of graphene. In fact, they can be readily prepared with high quality via well-established soft chemical routes. Though they are still far from being fully explored, in contrast to the current research boom on graphene and even metal dichalcogenides, they are being recognized and receiving renewed interest as an important class of 2D materials beyond graphene. This Account aims to offer a relatively up-to-date review of the research status of oxide and hydroxide nanosheets, focusing on their controllable preparation and mechanism of exfoliation, while also considering some aspects of their application as 2D building blocks for functional assemblies.

2. CONTROLLABLE PREPARATION OF HIGH-QUALITY NANOSHEETS

2.1. Layered Host Compounds for Exfoliation

The most effective route to preparing nanosheets is through the disintegration of a layered precursor compound. Layered compounds may be categorized into three types, based on the charge of the host layer: neutral, negatively charged, and positively charged. Figure 1 illustrates the crystal structures for some representative layered compounds, that is, neutral (e.g., graphite, hexagonal boron nitride (h-BN)), negatively charged (oxides), and positively charged (hydroxides). The tendency toward exfoliation arises from the unique structural characteristics of these layered compounds: strong covalent bonding in the host layer with relatively weaker layer-to-layer interactions, such as van der Waals or electrostatic attractive forces.

It is well known that graphene can be obtained by the micromechanical cleavage of graphite using the Scotch-tape process.¹ Though the procedure is time-consuming and the yield is low, it is the most straightforward method for producing the single-layer form of a layered crystallite while retaining the

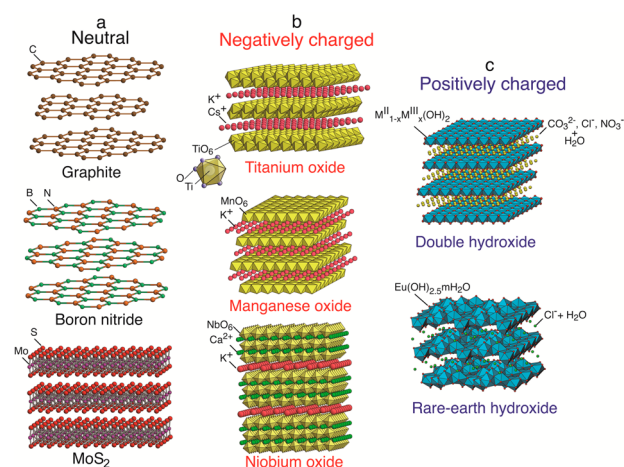


Figure 1. Layered compounds categorized by host layer charge. (a) Electrically neutral compounds (graphite, h-BN, and MoS₂), (b) negatively charged oxides (Cs_{0.7}Ti_{1.825}O₄ (or K_{0.8}Ti_{1.73}Li_{0.27}O₄), K_{0.45}MnO₂, and KCa₂Nb₃O₁₀), and (c) positively charged hydroxides (M²⁺_{1-x}M³⁺_x(OH)₂Aⁿ⁻_{x/n}mH₂O and RE(OH)_{2.5}mH₂O·Cl⁻_{0.5}).

intrinsic host structure. This method has also been successfully applied to dichalcogenides, for example, single-layer MoS₂ nanosheets.⁴ Very recently, a method of direct liquid exfoliation, involving exposing layered compounds to ultrasonic waves, was proposed for the facile production of nanosheets.^{20,21} The selection of a suitable solvent is a key to stabilize cleaved crystallites. Although this process is useful, the yield of unilamellar nanosheets is generally no more than a few tens of percent. In general, these two methods are typically employed to pick up individual 2D crystallites for the purpose of physical property evaluation. It would obviously be difficult to employ such samples as a starting material for the fabrication of functional nanostructured materials in a uniform bulk form.

For high-yield production of unilamellar 2D nanosheets, chemical or electrochemical redox protocols have been developed to charge the neutral host layer, allowing counter-ionic species to intercalate into the interlayer space, which may benefit exfoliation. For example, a chemical process known as the modified Hummers' method originated in the 1950s or 1960s involving the oxidation of graphite in the presence of strong acids/oxidants has gradually been accepted for the bulk production of graphene oxide (GO) and its reduction into graphene (i.e., reduced GO).^{22–24} Recently, the exfoliation procedure for MoS₂ developed in 1980s, involving reductive Li intercalation and subsequent reaction with water, has also been revisited and modified to produce high-quality dichalcogenide nanosheets.^{8,9,25}

On the other hand, most layered metal oxides and hydroxides accommodate interlayer exchangeable cations and anions, respectively, which can be effectively utilized for the purpose of delamination.^{12–14} Though it still lacks a general principle to distinguish the layered hosts that do or do not exfoliate, a soft chemical process has become well established to delaminate many layered hosts through the following steps: initial interlayer modification via ion-exchange, subsequent osmotic swelling, and exfoliation in a solution. The exfoliation is regarded as infinite swelling, or the ultimate consequence of the swelling accompanied by the inflow of a large amount of water or solvent, which significantly weakens the layer-to-layer attractive force. Recent studies have revealed some important and general insights into the process, especially into the

osmotic swelling stage largely unexplored until recently. The swelling and exfoliation seem to be affected by a series of factors, ranging from composition, charge density, and the counterionic species between layers to the nature of the exfoliating agent or solvent (size, polarity, dielectricity, etc.).^{26,27}

2.2. Soft Chemical Exfoliation: Ion-Exchange to Osmotic Swelling and Exfoliation

2.2.1. Oxide Nanosheets. The production of oxide nanosheets is illustrated for typical examples, $\text{Cs}_{0.7}\text{Ti}_{1.825}\text{O}_4$ (or $\text{K}_{0.8}\text{Ti}_{1.73}\text{Li}_{0.27}\text{O}_4$), $\text{K}_{0.45}\text{MnO}_2$, and $\text{KCa}_2\text{Nb}_3\text{O}_{10}$ (Figure 1b), which are composed of host slabs of corner- or edge-shared MO_6 octahedra (where $M = \text{Ti}, \text{Mn}, \text{Nb}, \text{etc.}$) and interlayer alkali metal cations ($\text{K}^+, \text{Rb}^+, \text{Cs}^+, \text{etc.}$).^{28–31} The polycrystalline sample of the parent layered materials can be synthesized by various methods, most typically, solid-state calcination at high temperature (800–1300 °C). Single crystal growth techniques, such as the flux method, can also be employed to produce single crystalline platelets of larger size. The layered compounds are converted into hydrated protonic forms, for example, $\text{H}_{0.7}\text{Ti}_{1.825}\text{O}_4 \cdot \text{H}_2\text{O}$ (or $\text{H}_{1.07}\text{Ti}_{1.73}\text{O}_4 \cdot \text{H}_2\text{O}$), $\text{H}_{0.13}\text{MnO}_2 \cdot 0.7\text{H}_2\text{O}$, and $\text{HCa}_2\text{Nb}_3\text{O}_{10} \cdot 1.5\text{H}_2\text{O}$, by treating with an acid solution. Due to their Brønsted solid acidity, the protons in the gallery can be further exchanged with organoammonium ions in an aqueous base solution, for example, tetrabutylammonium hydroxide (TBA^+OH^- , i.e., $(\text{C}_4\text{H}_9)_4\text{N}^+\text{OH}^-$). Such a reaction is frequently accompanied by the introduction of a massive volume of water, and the electrostatic interaction between host layers is significantly decreased. As a consequence, the swollen phases undergo exfoliation with the aid of a shearing force, for example, manual or mechanical shaking or ultrasonic agitation.

After exfoliation, well-dispersed unilamellar nanosheets, $\text{Ti}_{0.91}\text{O}_2^{0.36-}$ (or $\text{Ti}_{0.87}\text{O}_2^{0.52-}$), $\text{MnO}_2^{0.4-}$, or $\text{Ca}_2\text{Nb}_3\text{O}_{10}^{-}$, are usually obtained as a stable colloidal suspension. Figure 2a–c

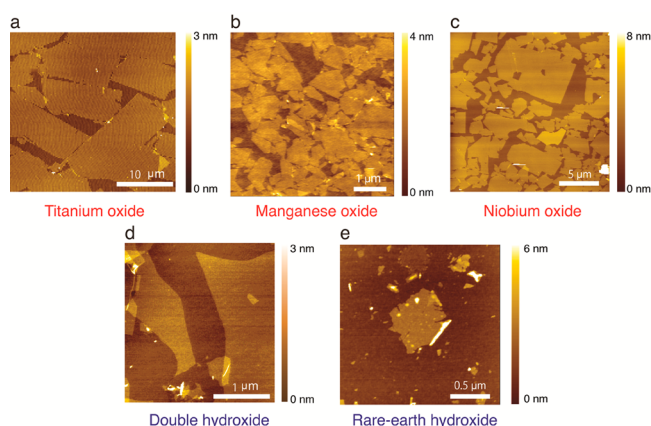


Figure 2. Representative AFM images of oxide and hydroxide nanosheets: (a) $\text{Ti}_{0.87}\text{O}_2^{0.52-}$; (b) $\text{MnO}_2^{0.4-}$; (c) $\text{Ca}_2\text{Nb}_3\text{O}_{10}^{-}$; (d) $[\text{Mg}_{2/3}\text{Al}_{1/3}(\text{OH})_2]^{1/3+}$; (e) $[\text{Eu}(\text{OH})_{2.3}m\text{H}_2\text{O}]^{0.5+}$. Reproduced from refs 14 and 36. Copyright 2010 John Wiley & Sons, Inc.

shows typical atomic force microscopy (AFM) images of $\text{Ti}_{0.87}\text{O}_2^{0.52-}$, $\text{MnO}_2^{0.4-}$, and $\text{Ca}_2\text{Nb}_3\text{O}_{10}^{-}$ nanosheets recorded from specimens obtained by drying the suspension on a Si substrate. Their measured thickness was ~ 1.2 , ~ 0.8 , and ~ 2.3 nm, respectively.^{28–31} These values are close to but somewhat larger than the crystallographic thicknesses of the host layers, possibly due to adsorbed water molecules at the surface. In

contrast, the lateral size of the nanosheets can vary from hundreds of nanometers to tens of micrometers, depending on the crystallite size of parent layered compounds as well as exfoliating conditions.

2.2.2. Hydroxide Nanosheets. As shown in Figure 1c, layered double hydroxides (LDHs) consist of octahedral hydroxide layers of divalent and trivalent (M^{2+} and M^{3+}) metal cations, accommodating charge-balancing anions (A^{n-}) in the interlayer gallery.^{13,14,18} They are represented by the general formula $\text{M}^{2+}_{1-x}\text{M}^{3+}_x(\text{OH})_2\text{A}^{n-}_{x/n} \cdot m\text{H}_2\text{O}$ (where $\text{M}^{2+} = \text{Mg}^{2+}, \text{Fe}^{2+}, \text{Co}^{2+}, \text{Ni}^{2+}, \text{Zn}^{2+}, \text{etc.}$; $\text{M}^{3+} = \text{Al}^{3+}, \text{Fe}^{3+}, \text{Co}^{3+}, \text{etc.}$; and $\text{A} = \text{CO}_3^{2-}, \text{Cl}^-, \text{NO}_3^-, \text{ClO}_4^-, \text{etc.}$). LDHs are routinely synthesized via the coprecipitation method, simply by mixing the constituent divalent and trivalent metal salts in an alkali solution. However, the product is usually a gel-like sample of low crystallinity. On the other hand, a so-called homogeneous precipitation from a mixed solution of MCl_2 and AlCl_3 using urea ($\text{CO}(\text{NH}_2)_2$) or hexamethylenetetramine (HMT, $\text{C}_6\text{H}_{12}\text{N}_4$) as a hydrolysis agent can produce uniform, hexagonally shaped LDH platelet crystals of micrometer width.^{13,32} Furthermore, a recently developed process involving the soft-chemical oxidation of homogeneously precipitated brucite-type $\text{M}^{2+}(\text{OH})_2$ (e.g., $\text{Co}_{1-x}\text{Fe}_x(\text{OH})_2$, $\text{Co}_{1-x}\text{Ni}_x(\text{OH})_2$) platelets can lead to highly crystalline all-transition-metal LDHs.³³ These newly developed synthetic methods have provided a convenient route to produce highly crystalline LDH samples suitable for controllable exfoliation. In pioneering studies, incorporation of some organophilic anions (amino acids, long-chain carboxylates, or other anionic surfactants) into LDHs was shown to effectively weaken the layer-to-layer interaction and facilitate swelling and exfoliation in some organic solvents. It was later discovered that well-crystallized LDH platelets in suitable inorganic anions (e.g., $\text{NO}_3^-, \text{ClO}_4^-, \text{etc.}$) could be swollen in formamide (HCONH_2) to be delaminated into well-defined single-layer nanosheets.^{13,14,32,33}

Recently, a new family of anion-exchangeable layered hydroxides, composed of positively charged hydroxide layers based on trivalent rare-earth cations, has been reported.^{17,34,35} Exfoliation of these new compounds has been achieved also in formamide after interlayer modification with dodecyl sulfate anions.³⁶

Figure 2d,e shows AFM images of the typical hydroxide nanosheets. Their estimated thicknesses of ~ 0.8 and ~ 1.6 nm, respectively, are again close to the crystallographic layer thicknesses of 0.48 and 0.93 nm of the precursor compounds.

To date, most of the hydroxide nanosheets were obtained in organic solvents.^{13,14} The recent report on substantial swelling of LDHs in water, after incorporation of aliphatic carboxylates or short-chain organic sulfonates (RSO_3^-), is encouraging for the development of new procedures to achieve hydroxide nanosheets in aqueous solutions.³⁷

2.2.3. Understanding Osmotic Swelling. As mentioned above, realizing a high degree of interlayer expansion, that is, gigantic osmotic swelling resulting from the penetration of a significant volume of solution, is a prerequisite to promote the exfoliation of layered oxides and hydroxides.^{12–14} A swelling–exfoliation scenario is schematically illustrated in Figure 3I. In principle, the swelling takes place in every interlayer gallery, eventually leading to the production of unilamellar nanosheets. In this context, the understanding of osmotic swelling is of critical importance to elucidate the mechanism of exfoliation and to achieve controllable preparation of high-quality

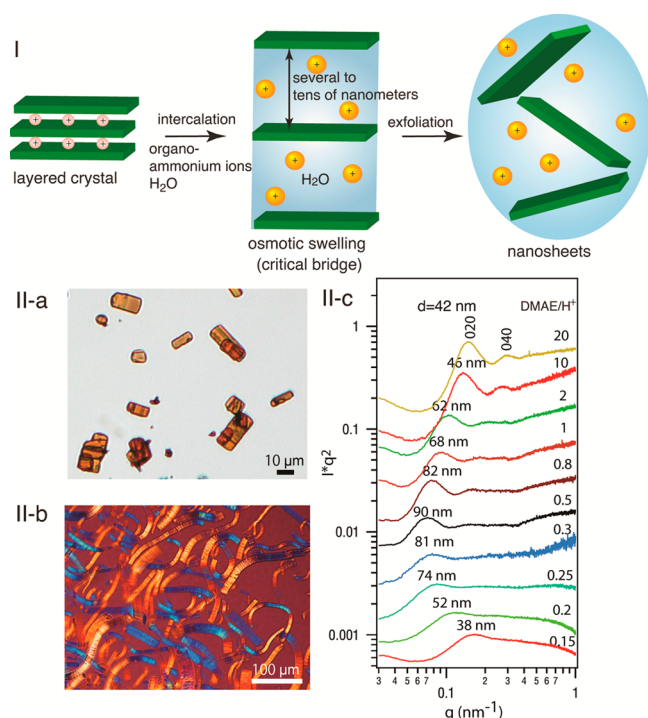


Figure 3. (I) Schematic illustration of the osmotic swelling to exfoliation process. Adapted from ref 27. Copyright 2014 American Chemical Society. (II-a) Optical microscopy image of platelet crystals of $\text{K}_{0.8}\text{Ti}_{1.2}\text{Fe}_{0.8}\text{O}_4$ with lateral sizes of $\sim 15 \times 35 \mu\text{m}^2$. The platelet thickness is $\sim 2\text{--}3 \mu\text{m}$, corresponding to stacks of ~ 3000 host layers. (II-b) Optical microscopy image of elongated crystals at maximum swelling in a diluted DMAE solution at $\text{DMAE}/\text{H}^+ = 0.5$ where H^+ denotes the amount of the exchangeable protons in the titanate. The longest swollen length is $\sim 200\text{--}250 \mu\text{m}$, corresponding to a nearly 100-fold expansion from the original thickness. (II-c) SAXS profiles of swollen phases with various ratios of DMAE/H^+ . The products of scattering intensity I and the inverse of the form factor of the flat thin sheet (q^2), I^*q^2 , are plotted against the scattering vector modulus, q . The lamellar period, $d (= 2\pi/q)$, first increases with increasing ratio of DMAE/H^+ , reaches a maximum spacing of $\sim 90 \text{ nm}$ at 0.5, and then begins decreasing with further increasing DMAE/H^+ . The measured maximum spacing of $\sim 90 \text{ nm}$ is consistent with ~ 100 -fold elongation of the crystal. Reproduced with permission from ref 26. Copyright 2013 Nature Publishing Group.

nanosheets. However, in general, such a high degree of swelling weakens the binding forces of neighboring layers so severely that they are prone to fall apart or spontaneously delaminate. In situ characterization of such a fragile swollen sample in abundant aqueous media is very difficult. These factors have prevented a deep understanding of the mechanism behind this intriguing and important reaction.

In recent studies, a surprisingly stable monolithic swelling of the layered oxides was found upon exposure to an aqueous solution of polar amine such as 2-(dimethylamino)ethanol (DMAE, $(\text{CH}_3)_2\text{NC}_2\text{H}_4\text{OH}$).^{26,27} Platelet crystals of $\text{H}_{0.8}\text{Ti}_{1.2}\text{Fe}_{0.4}\text{O}_4 \cdot \text{H}_2\text{O}$ undergo unidirectional swelling to ~ 100 times their original thickness (Figure 3II-a,b). The greatly elongated crystals were stable without noticeable collapse. Small angle X-ray scattering (SAXS) measurements confirm this enormous swelling, revealing a huge interlayer separation to $\sim 90 \text{ nm}$.²⁶ The greatly expanded gallery is filled almost exclusively with H_2O , with a trace amount of DMAE in a protonated form. It was found that a range of organo-ammonium ions induce similar massive swelling. Systematic

studies indicate that the uptake of ammonium ions into the layered protonated oxides is predominantly affected by the acid–base equilibrium, while the degree of swelling or inflow of H_2O is governed by the osmotic pressure balance between the inner gallery and the outer solution, both of which are relatively independent of amine identity but depend substantially on its molarity.²⁷ That is to say, the osmotic swelling process is essentially colligative in nature. On the other hand, the stability of the resultant swollen structure is strongly dependent on the chemical nature of the amines or ammonium ions. Species of higher polarity and smaller size, for example, DMAEH^+ , help stabilize the swollen structure, whereas those of lower polarity and bulky size, for example, TBA^+ or tetramethylammonium ion (TMA^+), are prone to trigger exfoliation. Such new insights provide fundamental scientific understanding of the long-standing mystery associated with osmotic swelling, as well as the exfoliation of layered compounds in general, rationalizing the selection of exfoliating reagents for the production of high-quality nanosheets.

2.3. Rational Design and Fine Control of Nanosheets

2.3.1. Control over Nanosheet Size. The nanosheet thickness is generally $0.5\text{--}4 \text{ nm}$, intrinsically dependent on the layer architecture of parent layered compounds, as far as delamination into elementary layers is ensured. In contrast, the lateral size of exfoliated nanosheets is variable, primarily determined by the crystal size of the precursor. It may also be affected by the mode of exfoliation (manual versus mechanical shaking, etc.). Exfoliation of polycrystalline samples by mechanical shaking usually brings about lateral fracture, yielding sub-micrometer to few micrometers-sized nanosheets. In contrast, exfoliation of a single crystal sample under gentle manual shaking can produce much larger nanosheets, as seen in $\text{Ti}_{0.87}\text{O}_2^{0.52-}$ nanosheets of several tens of micrometers (See Figure 2a).

The lateral size of the nanosheets could also be tuned by controlling the kinetics of the exfoliating reaction, for example, the type of amine/ammonium ions, their concentration, etc. Recently, the osmotic swelling and exfoliation behaviors of the protonated oxide $\text{H}_{1.07}\text{Ti}_{1.73}\text{O}_4 \cdot \text{H}_2\text{O}$, upon interaction with two typical tetraalkylammonium ions, TMA^+ and TBA^+ , was comparatively studied.³⁸ In the reaction with TMA^+ over a short time, few-layer flakes were obtained as a major product. Conversely, in the other case with TBA^+ , besides few-layer stacks, single-layer nanosheets were obtained as a major component. In both cases, unilamellar nanosheets were obtained after a sufficiently long shaking time. As shown in Figure 4, the nanosheets produced by TMA^+ generally exhibit larger lateral sizes, up to tens of micrometers, and the suspension showed a distinctively silky appearance, arising from the liquid crystallinity of 2D nanosheets of a high aspect ratio.

2.3.2. Fine Tuning of the Composition and Structure of Nanosheets. The rational design and tuning of the chemical composition and 2D structure of nanosheets are vital for developing diverse functionalities. Fortunately, the composition of nanosheets can be readily modified by element substitution or doping at the synthesis stage of the precursor layered compounds. The compositional and structural modification of parent layered compounds is well preserved in the exfoliated nanosheets. For example, oxide nanosheets with unique magnetic or photoluminescent properties have been

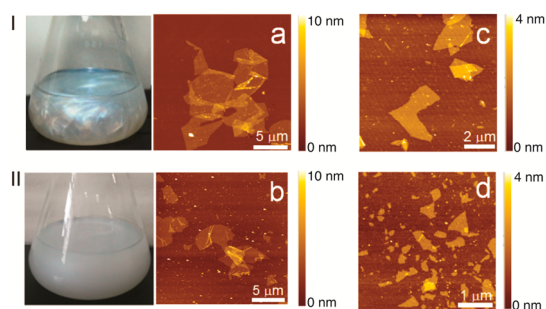


Figure 4. Control of the lateral size of nanosheets. Appearance of the nanosheet suspensions obtained at a TAA⁺/H⁺ ratio of 0.5: (I) TMA⁺; (II) TBA⁺. Typical AFM images of the unilamellar nanosheets: (a) TMA⁺ under manual shaking (18 weeks); (b) TBA⁺ under manual shaking (18 weeks); (c) TMA⁺ under mechanical shaking (1 week); (d) TBA⁺ under mechanical shaking (1 week). Reproduced with permission from ref 38. Copyright 2013 American Chemical Society.

obtained by doping with transition metal (e.g., Co, Fe, Mn) and rare-earth ions (e.g., Eu, Tb), respectively.^{14–16,19}

A favorable attribute of layered perovskite oxides stems from the high flexibility of their chemical composition and crystal structure, affording them a rich variety of electronic and magnetic properties. For example, Dion–Jacobson phases with the chemical formula $\text{KCa}_2\text{Na}_{n-3}\text{Nb}_n\text{O}_{3n+1}$ for $n = 3–7$ represent a homologous series, with the host layer thickness increasing stepwise by the number of NbO_6 octahedra, n , along the layer normal.³¹ In a recent study, these compounds were exfoliated via the standard soft chemical process to yield colloidal nanosheets.³⁹ AFM measurements confirmed the formation of micrometer-sized $\text{Ca}_2\text{Na}_{n-3}\text{Nb}_n\text{O}_{3n+1}$ nanosheets exhibiting a thickness of 2.3 nm ($n = 3$), 2.7 nm ($n = 4$), 3.1 nm ($n = 5$), and 3.6 nm ($n = 6$) (see Figure 5), which agree well with the homologous layer structure. These results demonstrate the successful preparation of a novel class of 2D perovskite-type oxide nanosheets with progressively increasing thicknesses at a step of 0.4–0.5 nm. Such precise control provides an ideal 2D system for studying structure–property relationships, for example, photocatalytic or dielectric properties as a function of the composition and thickness of ultrathin 2D oxide systems.

3. MOLECULAR ASSEMBLY AND EXPLORATION OF THE FUNCTIONALITY OF NANOSHEETS

3.1. Electrostatic Self-Assembly

Oxide and hydroxide nanosheets are both charge-bearing and monodispersed in colloidal suspensions. A range of functional materials or assemblies, such as nanocomposites and nanofilms, can be fabricated via solution-based processes, employing the nanosheets as 2D building blocks.^{12,14–16} In particular, electrostatic self-assembly, taking advantage of the charged feature, is a very convenient protocol. A multilayer film can be built up layer-by-layer by repeatedly dipping a substrate in first a polyelectrolyte solution and second the colloidal suspension of nanosheets. For negatively charged oxide nanosheets, polycations such as poly(diallyldimethylammonium chloride), polyethylenimine, Al_{13} Keggin ions, and other cationic metal complexes can be employed as counterparts in the film fabrication. For positively charged hydroxide nanosheets, polyanions such as poly(styrene 4-sulfonate) are widely selected as counterions. The regular multilayer buildup can be verified by various characterization techniques, including X-ray diffraction (XRD), UV–visible absorption spectra, ellipsometry, and so forth. Such a layer-by-layer assembly approach has been widely applied for the fabrication of multilayer nanostructured films of $\text{Ti}_{0.91}\text{O}_2^{0.36-}$ (or $\text{Ti}_{0.87}\text{O}_2^{0.52-}$), $\text{MnO}_2^{0.4-}$, $\text{Ca}_2\text{Nb}_3\text{O}_{10}^-$, $\text{Mg}^{2+}-\text{Al}^{3+}$, and $\text{Co}^{2+}-\text{Al}^{3+}$ LDH nanosheets, etc.^{12,14–16}

3.2. Langmuir–Blodgett Deposition

The Langmuir–Blodgett (LB) procedure is applicable for fabricating highly organized films of nanosheets. TBA⁺ ions in a colloidal suspension were found to support nanosheets spontaneously floating at the air/water interface, without the need for spreading an amphiphilic surfactant. The floating nanosheets can be suitably gathered or packed via surface compression, and then transferred onto a substrate. This LB transfer technique has been applied for nanofilm fabrication from a range of nanosheets, such as $\text{Ti}_{0.91}\text{O}_2^{0.36-}$ (or $\text{Ti}_{0.87}\text{O}_2^{0.52-}$), $\text{Ca}_2\text{Nb}_3\text{O}_{10}^-$, and $\text{La}_{0.90}\text{Eu}_{0.05}\text{Nb}_2\text{O}_7^-$.^{14,16} The nanosheets can be densely packed, without making gaps or overlaps, to produce better ordered mono- and multilayer nanostructures compared with the aforementioned electrostatic

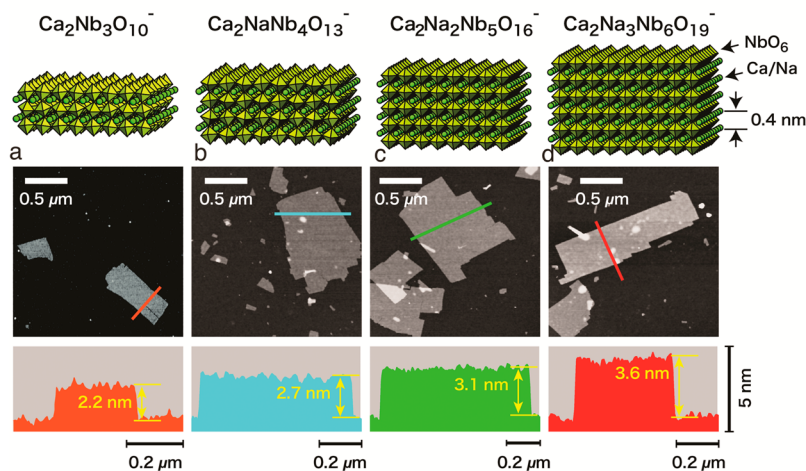


Figure 5. Control of the molecular thickness of nanosheets. Structure models (the sheets laterally extend to nearly infinity at this scale), AFM images, and height profiles for $\text{Ca}_2\text{Na}_{n-3}\text{Nb}_n\text{O}_{3n+1}$ nanosheets: (a) $n = 3$; (b) $n = 4$; (c) $n = 5$; (d) $n = 6$. Reproduced with permission from ref 39. Copyright 2012 American Chemical Society.

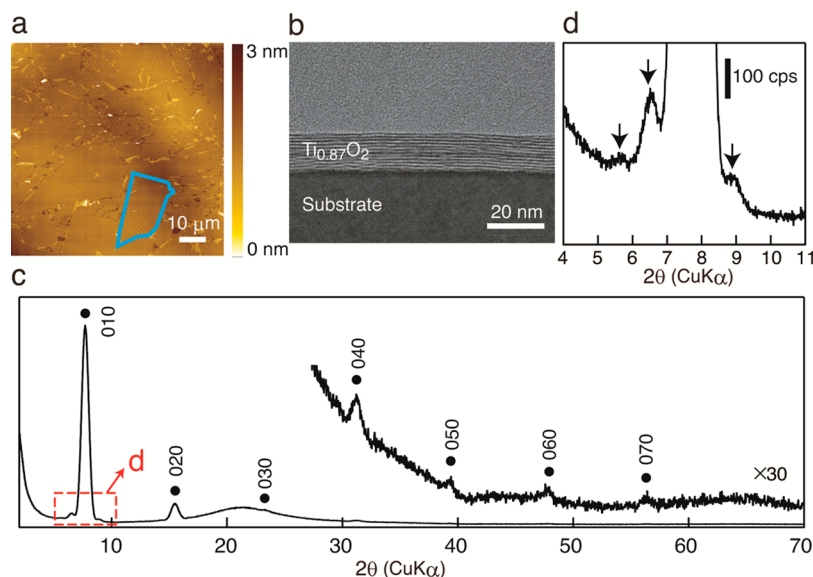


Figure 6. High-quality nanofilm composed of $\text{Ti}_{0.87}\text{O}_2^{0.52-}$ nanosheets fabricated by LB deposition. (a) AFM image of the film showing the neat packing of nanosheets. The blue outline indicates a selected individual nanosheet. (b) Cross-sectional high-resolution TEM image of a 10-layer film. (c) XRD pattern for the film with discernible $0k0$ basal reflections up to the seventh order. (d) Enlarged view of XRD profile of the 010 reflection, showing Laue ripples. Reproduced with permission from ref 40. Copyright 2009 American Chemical Society.

self-assembly procedure.⁴⁰ As depicted in Figure 6, $\text{Ti}_{0.87}\text{O}_2^{0.52-}$ nanosheets are neatly tiled on the substrate surface. Furthermore, cross-sectional transmission electron microscopy (TEM) imaging resolves a lamellar fringe of regularly stacked nanosheets. The corresponding XRD data displays sharp basal reflections of up to the seventh order. In addition, the first basal reflection is accompanied by small satellite peaks, which are accounted for by the Laue interference effect. All these characterizations identify the exceptionally well-ordered lamellar quality of the LB films, which is even comparable to artificial lattice films constructed via modern physical deposition techniques.

3.2. Exploration of Functionality for Various Applications

The molecular assemblies of nanosheets (nanocomposites, nanofilms, etc.) exhibit new or enhanced physicochemical functions.^{14–16,19} For example, titanium oxide nanosheet films show high UV-shielding properties.¹⁴ A 20-layer film of $\text{Ti}_{0.91}\text{O}_2^{0.36-}$ nanosheets, with a total thickness of ~ 20 nm, can attenuate UV irradiation at 265 nm to 5% of the incident intensity. A monolayer film of this nanosheet, just ~ 1 nm thick, can show very efficient photoinduced superhydrophilicity, almost comparable to a sol–gel-derived anatase film of a much greater thickness (>200 nm). Such a dramatic enhancement in surface properties can be ascribed to the discrete 2D nature of nanosheets.

Recent theoretical and experimental investigations have demonstrated that Ti- or Nb-based oxide nanosheets act as robust high- k dielectric nanoblocks.^{16,40} For example, multilayer nanofilms of $\text{Ti}_{0.87}\text{O}_2^{0.52-}$ nanosheets exhibit a high dielectric constant of ~ 125 at a thickness down to ~ 10 nm. Similarly, films of perovskite-type nanosheets such as $\text{Ca}_2\text{Nb}_3\text{O}_{10}^-$ demonstrate a high dielectric constant of >200 , the largest value reported so far in perovskite oxide films with a thickness as thin as ~ 10 nm.¹⁶ The solution-based deposition of nanosheets at room temperature achieves a good film-to-substrate interface, circumventing the formation of any interfacial dead layers, which has been a severe drawback in

physical deposition technology involving high-temperature operations. This process offers a unique route to the fabrication of superior high- k nanodielectrics.

One exciting application of 2D nanosheets is their use as a one-nanometer-thick seed layer for microepitaxial growth of various crystal films on conventional substrates such as glass.⁴¹ Nanosheets can promote the highly controlled, oriented film growth of materials, the structure of which matches the 2D lattice of the nanosheet. Because many nanosheets with various 2D structures are available, this technique can be applied for the orientation control and design of a range of functional crystal films. For the demonstration of feasibility, oriented growth of perovskite SrTiO_3 films (cubic, $a = 0.390$ nm) along the three important axes of (100), (110), and (111) was achieved on glass substrates covered with nanosheets of $\text{Ca}_2\text{Nb}_3\text{O}_{10}^-$ (2D square, $a = 0.386$ nm), $\text{Ti}_{0.87}\text{O}_2^{0.52-}$ (2D rectangular, $a = 0.376$ nm, $c = 0.297$ nm), and $\text{MoO}_2^{\delta-}$ (2D pseudo-hexagonal, $a = 0.290$ nm), respectively (Figure 7).⁴² In another study, tantalum oxide (TaO_3^-) nanosheets, a unique 2D mesh structure with opening channels that are almost the same size as the lithium ion, were deposited at the interface between a cathode material of LiCoO_2 and a thio-LISICON-type solid electrolyte. The resistance between these two materials was thereby decreased by 2 orders of magnitude, suggesting that TaO_3^- nanosheets prevent electronic conduction while allowing the penetration of lithium ions through the open channels.⁴³ This result will be useful for realizing high-performance all-solid-state lithium ion batteries.

More importantly, the heteroassembly of multiple nanosheets in a designed sequence can create artificial superlattice-like materials, which may evolve novel functionalities. For example, a superlattice film was constructed by alternately depositing semiconducting $\text{Ti}_{0.91}\text{O}_2^{0.36-}$ and redoxable $\text{MnO}_2^{0.4-}$ nanosheets.⁴⁴ The excitation of $\text{Ti}_{0.91}\text{O}_2^{0.36-}$ nanosheets under UV irradiation at 280 nm was found to bring about the reduction of Mn^{4+} to Mn^{3+} in $\text{MnO}_2^{0.4-}$ nanosheets, indicating that electrons excited in the $\text{Ti}_{0.91}\text{O}_2^{0.36-}$ are injected into adjacent $\text{MnO}_2^{0.4-}$ nanosheets. This activity may be

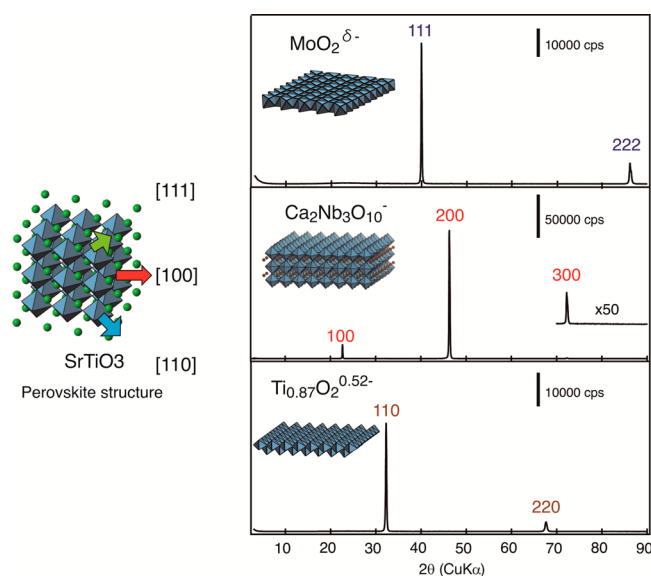


Figure 7. XRD data showing the orientation control of SrTiO₃ films along the (100), (110), and (111) axes. Ca₂Nb₃O₁₀⁻, Ti_{0.87}O₂^{0.52-}, and MoO₂^{δ-} nanosheets, respectively, are utilized as a seed layer. Adapted from ref 42 with permission of The Royal Society of Chemistry.

regarded as photochemical energy storage in the rationally designed heteroassembly. Recently, a superlattice system was fabricated using two paraelectric oxide nanosheets (LaNb₂O₇⁻ and Ca₂Nb₃O₁₀⁻) as building blocks.⁴⁵ Through such artificial structuring, the superlattice possesses a new form of interface coupling, which gives rise to robust ferroelectric properties at several nanometer thicknesses, the thinnest level reported so far. Interest in this area is rapidly growing, cultivating a research frontier of 2D materials.

4. SUMMARY AND OUTLOOK

In this Account, the current research status on 2D oxide and hydroxide nanosheets, especially the controllable preparation and new insight into the swelling and exfoliating mechanism, was reviewed. Utilizing these 2D nanosheets as building blocks, new and enhanced functionalities can be rationally designed through the elegant molecular assembly approach. This cutting-edge field of research is attracting more and more attention.

The ever-expanding nanosheet library, either through exfoliation of new functional layered compounds or through the development of new exfoliation methods, will certainly strengthen the position of 2D oxide and hydroxide nanosheets as alternatives to graphene. Future research requires the sophisticated tuning of chemical composition and structure desirable for a targeted functionality, as well as the further scale-up of the purity and yield of nanosheets, ideally the industrial-scale production of unilamellar nanosheets of large size and regular shape.

The solution-based molecular assembly using 2D oxide and hydroxide nanosheets as building blocks into high-quality nanofilms will be actively explored to realize novel functionalities that will be useful in next-generation electronic or optical devices, among others. This research will emphasize the promising potential for the design of heterostructures by integrating these oxide and hydroxide nanosheets with graphene or metal dichalcogenide sheets.

AUTHOR INFORMATION

Corresponding Author

*SASAKI.Takayoshi@nims.go.jp.

Notes

The authors declare no competing financial interest.

Biographies

Renzhi Ma received his Ph.D. degree in materials processing engineering from Tsinghua University (Beijing) in 2000. He then worked as a postdoctoral fellow for three years before becoming a staff scientist at the National Institute for Material Science (NIMS) in Japan. He is currently a MANA scientist at the International Center for Materials Nanoarchitectonics (MANA) at NIMS. His work focuses on the synthetic chemistry of inorganic nanotubes and nanosheets.

Takayoshi Sasaki received his Ph.D. in chemistry from the University of Tokyo in 1985. Since 1980, he has worked for the National Institute for Research in Inorganic Materials (NIRIM) in Japan, which is now the National Institute for Materials Science (NIMS). In 2009, he was appointed as a NIMS fellow. His recent research has focused on nanosheets obtained by delaminating layered materials.

REFERENCES

- (1) Novoselov, K. S.; Geim, A. K.; Morozov, S. V.; Jiang, D.; Katsnelson, M. I.; Grigorieva, I. V.; Dubonos, S. V.; Firsov, A. A. Two-dimensional gas of massless Dirac fermions in graphene. *Nature* **2005**, *438*, 197–200.
- (2) Novoselov, K. S.; Fal'ko, V. I.; Colombo, L.; Gellert, P. R.; Schwab, M. G.; Kim, K. A roadmap for graphene. *Nature* **2012**, *490*, 192–200.
- (3) Huang, X.; Qi, X.; Boey, F.; Zhang, H. Graphene-based composites. *Chem. Soc. Rev.* **2012**, *41*, 666–686.
- (4) Novoselov, K. S.; Jiang, D.; Schedin, F.; Booth, T. J.; Khotkevich, V. V.; Morozov, S. V.; Geim, A. K. Two-dimensional atomic crystals. *Proc. Natl. Acad. Sci. U. S. A.* **2005**, *102*, 10451–10453.
- (5) Geim, A. K.; Grigorieva, I. V. Van der Waals heterostructures. *Nature* **2013**, *499*, 419–425.
- (6) Butler, S. Z.; Hollen, S. M.; Cao, L.; Cui, Y.; Gupta, J. A.; Gutiérrez, H. R.; Heinz, T. F.; Hong, S. S.; Huang, J.; Ismach, A. F.; Johnston-Halperin, E.; Kuno, M.; Plashnitsa, V. V.; Robinson, R. D.; Ruoff, R. S.; Salahuddin, S.; Shan, J.; Shi, L.; Spencer, M. G.; Terrones, M.; Windl, W.; Goldberger, J. E. Progress, challenges, and opportunities in two-dimensional materials beyond graphene. *ACS Nano* **2013**, *7*, 2898–2926.
- (7) Xu, M. S.; Liang, T.; Shi, M. M.; Chen, H. Z. Graphene-like two-dimensional materials. *Chem. Rev.* **2013**, *113*, 3766–3798.
- (8) Huang, X.; Zeng, Z. Y.; Zhang, H. Metal dichalcogenide nanosheets: Preparation, properties and applications. *Chem. Soc. Rev.* **2013**, *42*, 1934–1946.
- (9) Chhowalla, M.; Shin, H. S.; Eda, G.; Li, L.-J.; Loh, K. P.; Zhang, H. The chemistry of two-dimensional layered transition metal dichalcogenide nanosheets. *Nat. Chem.* **2013**, *5*, 263–275.
- (10) Wang, Q. H.; Kalantar-Zadeh, K.; Kis, A.; Coleman, J. N.; Strano, M. S. Electronics and optoelectronics of two-dimensional transition metal dichalcogenides. *Nat. Nanotechnol.* **2012**, *7*, 699–712.
- (11) Li, H.; Wu, J.; Yin, Z.; Zhan, H. Preparation and applications of mechanically exfoliated single-layer and multilayer MoS₂ and WS₂ nanosheets. *Acc. Chem. Res.* **2014**, *47*, 1067–1075.
- (12) Sasaki, T. Fabrication of nanostructured functional materials using exfoliated nanosheets as a building block. *J. Ceram. Soc. Jpn.* **2007**, *115*, 9–16.
- (13) Ma, R.; Liu, Z.; Li, L.; Iyi, N.; Sasaki, T. Exfoliating layered double hydroxides in formamide: A method to obtain positively charged nanosheets. *J. Mater. Chem.* **2006**, *16*, 3809–3813.

- (14) Ma, R.; Sasaki, T. Nanosheets of oxides and hydroxides: Ultimate 2D charge-bearing functional crystallites. *Adv. Mater.* **2010**, *22*, 5082–5104.
- (15) Osada, M.; Sasaki, T. Exfoliated oxide nanosheets: New solution to nanoelectronics. *J. Mater. Chem.* **2009**, *19*, 2503–2511.
- (16) Osada, M.; Sasaki, T. Two-dimensional dielectric nanosheets: Novel nanoelectronics from nanocrystal building blocks. *Adv. Mater.* **2012**, *24*, 210–228.
- (17) Geng, F.; Ma, R.; Sasaki, T. Anion-exchangeable layered materials based on rare-earth phosphors: Unique combination of rare-earth host and exchangeable anions. *Acc. Chem. Res.* **2010**, *43*, 1177–1185.
- (18) Wang, Q.; O'Hare, D. Recent advances in the synthesis and application of layered double hydroxide (LDH) nanosheets. *Chem. Rev.* **2012**, *112*, 4124–4155.
- (19) Wang, L.; Sasaki, T. Titanium oxide nanosheets: Graphene analogues with versatile functionalities. *Chem. Rev.* **2014**, *114*, 9455–9486.
- (20) Coleman, J. N.; Lotya, M.; O'Neill, A.; Bergin, S. D.; King, P. J.; Khan, U.; Young, K.; Gaucher, A.; De, S.; Smith, R. J.; Shvets, I. V.; Arora, S. K.; Stanton, G.; Kim, H. Y.; Lee, K.; Kim, G. T.; Duesberg, G. S.; Hallam, T.; Boland, J. J.; Wang, J. J.; Donegan, J. F.; Grunlan, J. C.; Moriarty, G.; Shmeliov, A.; Nicholls, R. J.; Perkins, J. M.; Grievson, E. M.; Theuvsen, K.; McComb, D. W.; Nellist, P. D.; Nicolosi, V. Two-dimensional nanosheets produced by liquid exfoliation of layered materials. *Science* **2011**, *331*, 568–571.
- (21) Nicolosi, V.; Chhowalla, M.; Kanatzidis, M. G.; Strano, M. S.; Coleman, J. N. Liquid exfoliation of layered materials. *Science* **2013**, *340*, No. 6139, DOI: 10.1126/science.1226419.
- (22) Park, S.; Ruoff, R. S. Chemical methods for the production of graphenes. *Nat. Nanotechnol.* **2009**, *4*, 217–224.
- (23) Eda, G.; Chhowalla, M. Chemically derived graphene oxide: Towards large-area thin-film electronics and optoelectronics. *Adv. Mater.* **2010**, *22*, 2392–2415.
- (24) Hummers, W. S.; Offeman, R. E. Preparation of graphitic oxide. *J. Am. Chem. Soc.* **1958**, *80*, 1339–1339.
- (25) Joensen, P.; Frindt, R. F.; Morrison, S. R. Single-layer MoS₂. *Mater. Res. Bull.* **1986**, *21*, 457–461.
- (26) Geng, F.; Ma, R.; Nakamura, A.; Akatsuka, K.; Ebina, Y.; Yamauchi, Y.; Miyamoto, N.; Tateyama, Y.; Sasaki, T. Unusually stable ~100-fold reversible and instantaneous swelling of inorganic layered materials. *Nat. Commun.* **2013**, *4*, No. 1632, DOI: 10.1038/ncomms2641.
- (27) Geng, F.; Ma, R.; Ebina, Y.; Yamauchi, Y.; Miyamoto, N.; Sasaki, T. Gigantic swelling of inorganic layered materials: A bridge to molecularly thin two-dimensional nanosheets. *J. Am. Chem. Soc.* **2014**, *136*, 5491–5500.
- (28) Sasaki, T.; Watanabe, M.; Hashizume, H.; Yamada, H.; Nakazawa, H. Macromolecule-like aspects for a colloidal suspension of an exfoliated titanate. Pairwise association of nanosheets and dynamic reassembling process initiated from it. *J. Am. Chem. Soc.* **1996**, *118*, 8329–8335.
- (29) Omomo, Y.; Sasaki, T.; Wang, L.; Watanabe, M. Redoxable nanosheet crystallites of MnO₂ derived via delamination of a layered manganese oxide. *J. Am. Chem. Soc.* **2003**, *125*, 3568–3575.
- (30) Liu, Z. P.; Ma, R.; Ebina, Y.; Takada, K.; Sasaki, T. Synthesis and delamination of layered manganese oxide nanobelts. *Chem. Mater.* **2007**, *19*, 6504–6512.
- (31) Ebina, Y.; Sasaki, T.; Watanabe, M. Study on exfoliation of layered perovskite-type niobates. *Solid State Ionics* **2002**, *151*, 177–182.
- (32) Liu, Z. P.; Ma, R.; Osada, M.; Iyi, N.; Ebina, Y.; Takada, K.; Sasaki, T. Synthesis, anion exchange, and delamination of Co-Al layered double hydroxide: Assembly of the exfoliated nanosheet/polyanion composite films and magneto-optical studies. *J. Am. Chem. Soc.* **2006**, *128*, 4872–4880.
- (33) Ma, R.; Liu, Z.; Takada, K.; Iyi, N.; Bando, Y.; Sasaki, T. Synthesis and exfoliation of Co²⁺-Fe³⁺ layered double hydroxides: An innovative topochemical approach. *J. Am. Chem. Soc.* **2007**, *129*, 5257–5263.
- (34) McIntyre, L. J.; Jackson, L. K.; Fogg, A. M. Ln₂(OH)₅NO₃·xH₂O (Ln = Y, Gd–Lu): A novel family of anion exchange intercalation hosts. *Chem. Mater.* **2008**, *20*, 335–340.
- (35) Geng, F.; Matsushita, Y.; Ma, R.; Xin, H.; Tanaka, M.; Izumi, F.; Iyi, N.; Sasaki, T. General synthesis and structural evolution of a layered family of Ln₈(OH)₂₀Cl₄·nH₂O (Ln = Nd, Sm, Eu, Gd, Tb, Dy, Ho, Er, Tm, and Y). *J. Am. Chem. Soc.* **2008**, *130*, 16344–16350.
- (36) Hu, L.; Ma, R.; Ozawa, T. C.; Sasaki, T. Exfoliation of layered europium hydroxide into unilamellar nanosheets. *Chem. Asian J.* **2010**, *5*, 248–251.
- (37) Iyi, N.; Ebina, Y.; Sasaki, T. Synthesis and characterization of water-swellaible LDH (layered double hydroxide) hybrids containing sulfonate-type intercalant. *J. Mater. Chem.* **2011**, *21*, 8085–8095.
- (38) Maluangnont, T.; Matsuba, K.; Geng, F.; Ma, R.; Yamauchi, Y.; Sasaki, T. Osmotic swelling of layered compounds as a route to producing high-quality two-dimensional materials. A comparative study of tetramethylammonium versus tetrabutylammonium cation in a lepidocrocite-type titanate. *Chem. Mater.* **2013**, *25*, 3137–3146.
- (39) Ebina, Y.; Akatsuka, K.; Fukuda, K.; Sasaki, T. Synthesis and in situ X-ray diffraction characterization of two-dimensional perovskite-type oxide colloids with a controlled molecular thickness. *Chem. Mater.* **2012**, *24*, 4201–4208.
- (40) Akatsuka, K.; Haga, M.; Ebina, Y.; Osada, M.; Fukuda, K.; Sasaki, T. Construction of highly ordered lamellar nanostructures through Langmuir-Blodgett deposition of molecularly thin titania nanosheets tens of micrometers wide and their excellent dielectric properties. *ACS Nano* **2009**, *3*, 1097–1106.
- (41) Shibata, T.; Fukuda, K.; Ebina, Y.; Kogure, T.; Sasaki, T. One-nanometer-thick seed layer of unilamellar nanosheets promotes oriented growth of oxide crystal films. *Adv. Mater.* **2008**, *20*, 231–235.
- (42) Shibata, T.; Takano, H.; Ebina, Y.; Kim, D. S.; Ozawa, T. C.; Akatsuka, K.; Ohnishi, T.; Takada, K.; Kogure, T.; Sasaki, T. Versatile van der Waals epitaxy-like growth of crystal films using two-dimensional nanosheets as a seed layer: orientation tuning of SrTiO₃ films along three important axes on glass substrates. *J. Mater. Chem. C* **2014**, *2*, 441–449.
- (43) Xu, X.; Takada, K.; Fukuda, K.; Ohnishi, T.; Akatsuka, K.; Osada, M.; Hang, B. T.; Kumagai, K.; Sekiguchi, T.; Sasaki, T. Tantalum oxide nanomesh as self-standing one nanometre thick electrolyte. *Energy Environ. Sci.* **2011**, *4*, 3509–3512.
- (44) Sakai, N.; Fukuda, K.; Omomo, Y.; Ebina, Y.; Takada, K.; Sasaki, T. Hetero-nanostructured films of titanium and manganese oxide nanosheets: Photoinduced charge transfer and electrochemical properties. *J. Phys. Chem. C* **2008**, *112*, 5197–5202.
- (45) Li, B.-W.; Osada, M.; Ozawa, T. C.; Ebina, Y.; Akatsuka, K.; Ma, R.; Funakubo, H.; Sasaki, T. Engineered interfaces of artificial perovskite oxide superlattices via nanosheet deposition process. *ACS Nano* **2010**, *4*, 6673–6680.